Finite Element Legendre Wavelet Galerkin Approch to Inward Solidification in Simple Body Under Most Generalized Boundary Condition

Sarita Yadav[a], Dinesh Kumar[b], and Kabindra Nath Rai[a,b]

[a] Department of Mathematical Sciences, Indian Institute of Technology (BHU), Varanasi-221005, Uttar Pradesh, India

[b] DST-CIMS, Faculty of Science, Banaras Hindu University, Varanasi-221005, Uttar Pradesh, India

Reprint requests to S. Y.; E-mail: syadav.rs.apm@itbhu.ac.in

Z. Naturforsch. **69a**, 501 – 510 (2014) / DOI: 10.5560/ZNA.2014-0052
Received March 27, 2014 / published online September 10, 2014

This paper deals with a mathematical model describing the inward solidification of a melt of phase change material within a container of different geometrical configuration like slab, circular cylinder or sphere under the most generalized boundary conditions. The thermal and physical properties of melt and solid are assumed to be identical. To solve this mathematical model, the finite difference scheme is used to convert the problem into an initial value problem of vector matrix form and further, solving it using the Legendre wavelet Galerkin method. The results thus obtained are analyzed by considering particular cases when one might impose either a constant/time varying temperature or a constant/time varying heat flux or a constant heat transfer coefficient on the surface. The whole analysis is presented in dimensionless form. The effect of variability of shape factor, condition posed at the boundary, Stefan number, Predvoditelev number, Kirpichev number, and Biot number on dimensionless temperature and solid-layer thickness are shown graphically. Furthermore, a comparative study of time for complete solidification is presented.

Key words: Moving Boundary Problem; Predvoditelev Number; Biot Number; Kirpichev Number; Finite Element Legendre Wavelet Galerkin Method (FELWGM).

1. Introduction

Modern technology demands to prepare a high strength material with exceptionally superior tensile properties, but at low cost. The most attractive method of producing such materials is through unidirectional solidification. A desired type of microstructure can be obtained by controlling the freezing conditions and adding a small quantity of impurity elements. The microstructure of eutectic alloys also depends on the rate of freezing. When ZrO_2-MgO eutectic freezes [1] at a growth rate of 8.9 cm/h, a cellular structure is formed whereas at a growth rate of 1 cm/h, the microstructure of ZrO_2-MgO eutectic is fully aligned with MgO rods in a cubic ZrO_2 matrix. At slow growth rates, Al_2O_3-UO_2 forms a rod eutectic, but at higher growth rates, the UO_2 rods tend to form a lamellar structure. The rate of freezing which controls the structure depends on a number of parameters. In order to determine the effect of these parameters on the rate of freezing, it is desirable to develop a generalized theoretical model which may predict transport phenomena during the solidification.

Industrial thermal processes where energy availability and its utilization are not coincident require a means of matching the use of energy with its availability. One can include the sensible and latent heat concepts of energy storage. Because of the large storage capacity and constant charge and discharge temperature, the latent heat concept is more attractive. The cool thermal storage systems include liquid–solid phase change materials encapsulated in containers of different geometrical shape. Understanding the thermal behaviour during phase change in the container, it is important to design efficient storage systems. The solidification which has immense technological importance mathematically occurs in a class of problems commonly known as moving boundary problems. The study of these problems is not simple as the freezing front is not known in advance, and along the freezing front temperature gradients are discontinuous. A good account of the analytical and numerical solutions of these problems can be found in a book by Crank [2].

Tien and Geiger [3], Carslaw and Jaegar [4], Ozisik [5], Hill [6], Viskanta [7] and Barry and

Goodling [8] also studied solidification problems from a heat transfer point of view. None of these authors studied inward solidification within a container filled with melt of phase change material. Goodling and Khader [9] obtained numerical solutions for the one-phase one-dimensional inward solidification problem with radiation-convection boundary condition. Gupta and Arora [10] obtained analytical and numerical solutions of the inward spherical solidification of a superheated melt with radiative-convective heat transfer and density jump at the freezing front. Yan and Huang [11] used a perturbation solution for one-phase slab problems. Shih and Chou [12] presented an iterative method of successive approximations to study the solidification process inside a spherical geometry. Rai and Rai [13] used the finite difference method to solve a problem of inward solidification of slabs, cylinder, and sphere. The solution of this problem is found in terms of eigenvalues and spectral component of the operator. Hill and Kucera [14] developed a semi-analytical method to study the solidification inside spherical containers taking into account the effects of heat radiation on the container surface. They estimated the time for complete solidification of the sphere. Ismail and Henriquez [15] presented a numerical study of the solidification of phase change material (PCM) enclosed in a spherical shell. Bilir and Zafer [16] investigated the inward solidification problem of PCM encapsulated in cylindrical or spherical containers. Chan and Tan [17] carried out an experimental study of the solidification of an *n*-hexadecane inside a spherical container. In case of inward solidification, the effect of shape factor of the container containing the melt and the condition posed on the boundary are not discussed in detail.

In present paper, a model describing the solidification of a melt within a container of geometrical configuration like slab, circular cylinder or sphere when its surface is subjected to the most generalized boundary conditions is presented. Initially, the melt is at its freezing temperature. Several assumptions have to be taken at the surfaces from which solidification commences. Such as constant/time varying container surface temperature, constant/time varying heat flux at the container surface, and constant convective heat transfer coefficient between the container surface and the surrounding medium. To solve this model, we have used the finite element Legendre wavelet Galerkin method (FELWGM) for finding the temperature and position of the moving interface. Furthermore, the effect of parameters such as Predvoditelev number, Kirpichev number, Biot number, and Stefan number on the moving layer thickness is discussed in detail.

2. Formulation of the Problem

A liquid phase change material contained either in a finite slab of thickness $2R$ or a cylinder or a sphere of diameter $2R$ is initially at its freezing temperature T_{f}. After time $t > 0$, the boundary is cooled by imposing on it the boundary condition of first kind or second kind or third kind. Namely, one might assume either a constant temperature $T_{\mathrm{w}} < T_{\mathrm{f}}$ (suscript w stands for wall and f stands for freezing) or a constant heat flux q or a constant heat transfer coefficient α. It is supposed that: (i) heat transfer occurs only in the r-direction; (ii) the container walls are so thin and of a so conductive material that the thermal resistance through the walls is negligible, the fact which is confirmed experimentally by Tan and Leong [18]; (iii) the mass densities of solid and liquid phases are equal. The melt freezes inward and the solidification shell grows in a symmetric manner. The finite region is divided into two regions separated by the solidification front $r = \lambda_0(t)$. The first region $\lambda_0(t) < r < R$ is in frozen form while the region $0 < r < \lambda_0(t)$ is in liquid form. The dynamics of freezing can be described by the following equations:

$$\frac{\partial T}{\partial t} = \frac{a}{r^{\Gamma}} \frac{\partial}{\partial r} \left(r^{\Gamma} \frac{\partial T}{\partial r} \right), \quad 0 < r < R, \quad t > 0, \tag{1}$$

where T is the temperature, a the thermal diffusivity, r the position of the solidification material, and $\Gamma = 0, 1, 2$ for a slab, cylinder, and spherical configuration, respectively. The initial condition and associated boundary conditions are

$$T(r,t) = T_{\mathrm{f}}, \quad t = 0, \tag{2}$$

$$A_0 \frac{\partial T}{\partial r} + B_0 T = f_0(t), \quad r = R, \quad t > 0, \tag{3}$$

where

$$\begin{aligned} &\text{(i)} \quad A_0 = 0, \quad B_0 = 1, \quad f_0(t) = T_{\mathrm{w}}, \\ &\text{(ii)} \quad A_0 = -K, \quad B_0 = 0, \quad f_0(t) = q, \\ &\text{(iii)} \quad A_0 = -K, \quad B_0 = \alpha, \quad f_0(t) = -\alpha T_{\infty}, \end{aligned}$$

are defined in first, second, and third kind of boundary condition, respectively. K is the thermal conductivity, q the heat flux at the wall, and α the convective heat

transfer coefficient. The energy balance at the solid-liquid interface is

$$\frac{\mathrm{d}(\lambda_0(t))}{\mathrm{d}t} = \frac{K}{\rho L}\frac{\partial T}{\partial r}, \quad r = \lambda_0(t), \tag{4}$$

$$\lambda_0(t) = 0, \quad r = R, \tag{5}$$

$$T(r,t) = T_\mathrm{f}, \quad r = \lambda_0(t), \tag{6}$$

where ρ is the density, L the latent heat of fusion, and $\lambda_0(t)$ the thickness of moving layer.

3. Solution of the Problem

Introducing the dimensionless variables and similarity criteria defined as

$$x = \frac{r}{R}, \quad S = \frac{C\Delta T}{L}, \quad \lambda = \frac{\lambda_0(t)}{R}, \quad \mathrm{Fo} = \frac{at}{R^2}, \quad \theta = \frac{(T - T_0)}{\Delta T}, \tag{7}$$

where

$$\text{(i)} \quad \Delta T = T_\mathrm{f} - T_\mathrm{w}, \quad T_0 = T_\mathrm{w}, \tag{8}$$

$$\text{(ii)} \quad \Delta T = \frac{ql}{K}, \quad T_0 = T_\mathrm{f} - \Delta T, \tag{9}$$

$$\text{(iii)} \quad \Delta T = T_\mathrm{f} - T_\infty, \quad T_0 = T_\infty, \tag{10}$$

in first, second, and third kind of boundary conditions, respectively. x is the dimensionless space coordinate, S the Stefan number, λ the dimensionless phase change front, Fo the solidification time, and θ the dimensionless temperature. Further

$$A' = \frac{A_0}{R}, \quad B' = B_0, \quad \theta_\mathrm{c}(\mathrm{Fo}) = \frac{\mathrm{Fo}(t) - B_0 T_0}{\Delta T}.$$

The system of (1)–(6) reduce into the dimensionless form as follows:

$$\frac{\partial \theta}{\partial \mathrm{Fo}} = \frac{a}{x^\Gamma}\frac{\partial}{\partial x}\left(x^\Gamma \frac{\partial \theta}{\partial x}\right), \quad 0 < x < 1, \ \mathrm{Fo} > 0 \tag{11}$$

$$A'\frac{\partial \theta}{\partial x} + B'\theta = \theta_\mathrm{c}(\mathrm{Fo}), \quad x = 1, \ \mathrm{Fo} > 0, \tag{12}$$

$$\theta(x,\mathrm{Fo}) = 1, \quad x = \lambda(\mathrm{Fo}), \tag{13}$$

$$\frac{\mathrm{d}\lambda(\mathrm{Fo})}{\mathrm{dFo}} = S\frac{\partial \theta}{\partial x}, \quad x = \lambda(\mathrm{Fo}), \tag{14}$$

$$\lambda(0) = 0, \tag{15}$$

$$\theta(x,0) = 1. \tag{16}$$

Replacing the domain $[1,0] \times [0,\infty]$ by a rectangular grid of points (x_i, Fo_i). We first deal with the discretization in the space variable by using central differences, then (11)–(13) and (16) can be written in vector matrix form as follows:

$$\frac{\mathrm{d}\theta}{\mathrm{dFo}} = A\theta + B, \tag{17}$$

and the initial condition is

$$\theta(0) = \begin{bmatrix} 1 & 1 & \cdots & \cdots & 1 \end{bmatrix}^\mathrm{T}. \tag{18}$$

Here

$$\theta(\mathrm{Fo}) = \begin{bmatrix} \theta_1 & \theta_2 & \cdots & \cdots & \theta_k \end{bmatrix}^\mathrm{T},$$

$$A = \frac{1}{2Sh^2} \cdot \begin{bmatrix} \frac{13A'\left(\frac{\Gamma h}{x_1}-2\right)}{(20hB'-21A')} - 4 & \frac{17A'\left(\frac{\Gamma h}{x_1}-2\right)}{(20hB'-21A')} + \left(\frac{\Gamma h}{x_1}+2\right) & \frac{-9A'\left(\frac{\Gamma h}{x_1}-2\right)}{(20hB'-21A')} & 0 & & 0 & 0 \\ \left(-\frac{\Gamma h}{x_2}+2\right) & -4 & \left(\frac{\Gamma h}{x_2}+2\right) & 0 & \cdots & 0 & 0 \\ 0 & \left(-\frac{\Gamma h}{x_3}+2\right) & -4 & \left(\frac{\Gamma h}{x_3}+2\right) & & 0 & 0 \\ 0 & 0 & \left(-\frac{\Gamma h}{x_4}+2\right) & -4 & & 0 & 0 \\ & \vdots & & & \ddots & \vdots & \\ 0 & 0 & 0 & 0 & & -4 & \left(\frac{\Gamma h}{x_{k-1}}+2\right) \\ 0 & 0 & 0 & 0 & \cdots & \left(\frac{\Gamma h}{x_k}+2\right) & -4 \end{bmatrix},$$

$$B = \frac{1}{2Sh^2}\begin{bmatrix} 20h & \frac{\left(-\frac{\Gamma h}{x_1}+2\right)\theta_\mathrm{c}(\mathrm{Fo})}{20hB'-21A'} & 0 & 0 & \cdots & \cdots & \left(\frac{\Gamma h}{x_k}+2\right) \end{bmatrix}^\mathrm{T}.$$

4. Finite Element Legendre Wavelet Galerkin Method

To solve the differential equation (17) under initial condition (18), let us assume that

$$\frac{\mathrm{d}\theta}{\mathrm{dFo}} = X\psi, \tag{19}$$

where X is an unknown $2^{k-1}M \times 2^{k'-1}M'$ $(M' \le M,$ $k' \le k)$ matrix, and ψ is a $2^{k-1}M \times 1$ matrix defined as

$$\Psi(\mathrm{Fo}) = \left[\Psi_{10}(\mathrm{Fo}), \Psi_{11}(\mathrm{Fo}), \cdots \Psi_{1M-1}(\mathrm{Fo}), \Psi_{20}(\mathrm{Fo}), \cdots \Psi_{2M-1}(\mathrm{Fo}), \cdots \Psi_{2^{k-1}0}(\mathrm{Fo}) \ldots \Psi_{2^{k-1}M-1}(\mathrm{Fo})\right]^{\mathrm{T}}. \tag{20}$$

The Legendre wavelets [19] $\psi_{nm}(\tau)$ are defined as

$$\psi_{nm}(\tau) = \begin{cases} \sqrt{\left(m+\frac{1}{2}\right)} 2^{\frac{k}{2}} P_m\left(2^k\tau - \hat{n}\right), \\ \quad \frac{\hat{n}-1}{2^k} \le \tau \le \frac{\hat{n}+1}{2^k}, \\ 0, \ \text{otherwise}, \end{cases} \tag{21}$$

where $k = 1,2,3\ldots$, $n = 1,2,\ldots,2^{k-1}$, $\hat{n} = (2n-1)$, m is the order of Legendre polynomial, and τ is the normalized time. They are defined on the interval $[0,1]$. $P_m(\tau)$ is denoted by Legendre polynomials of order m which are orthogonal with respect to the weight function $w(\tau) = 1$, $\tau \in [-1,1]$.

Integrating the above differential equation from 0 to Fo and the using initial condition, we get

$$\theta = \theta(0) + XP\psi, \tag{22}$$

where P is an operational matrix of order $2^{k-1}M \times 2^{k-1}M$. The operational matrix of integration [20] is defined as

$$\int_0^\tau \psi(s)\,\mathrm{d}s = P\psi(\tau), \ \ \tau \in [0,1], \tag{23}$$

$$P = \frac{1}{2^k}\begin{pmatrix} L & O & O & \ldots & O \\ 0 & L & O & \ldots & O \\ 0 & 0 & L & \ldots & O \\ \vdots & \vdots & \vdots & \ddots & \vdots \\ 0 & 0 & 0 & \ldots & O \\ 0 & 0 & 0 & \ldots & O \end{pmatrix}, \tag{24}$$

where O and L are $M \times M$ matrices given by

$$O = \begin{pmatrix} 2 & 0 & \ldots & 0 \\ 0 & \vdots & \ldots & \vdots \\ \vdots & \vdots & \ddots & \vdots \\ 0 & 0 & \ldots & 0 \end{pmatrix}$$

and

$$L = \begin{bmatrix} 1 & \frac{1}{\sqrt{3}} & 0 & 0 & & 0 & 0 \\ \frac{-1}{\sqrt{3}} & 0 & \frac{1}{\sqrt{15}} & 0 & \ldots & 0 & 0 \\ 0 & \frac{-1}{\sqrt{15}} & 0 & \frac{1}{\sqrt{35}} & & 0 & 0 \\ 0 & 0 & \frac{-1}{\sqrt{35}} & 0 & & 0 & 0 \\ & \vdots & & & \ddots & \vdots & \\ 0 & 0 & 0 & 0 & & 0 & \frac{\sqrt{2M-3}}{(2M-3)\sqrt{2M-1}} \\ 0 & 0 & 0 & 0 & \ldots & \frac{-\sqrt{2M-1}}{(2M-1)\sqrt{2M-3}} & 0 \end{bmatrix}.$$

Substituting this value of $\theta(\mathrm{Fo})$ in the differential equation (17), we get

$$X\psi = A(\theta(0) + XP\psi) + B, \tag{25}$$

$$AXP\psi - X\psi + A\theta(0)d^T\psi + Bd^{\mathrm{T}}\psi = 0, \tag{26}$$

where $d^{\mathrm{T}}\psi = 1$.

The above equation reduces in the form of

$$AXP - X + (A\theta(0) + B)d^{\mathrm{T}} = 0. \tag{27}$$

Let $N = (A\theta(0) + B)d^{\mathrm{T}}$, then the above system reduces to

$$AXP - X + N = 0. \tag{28}$$

We look for the generalized time Fo in which the interface moves a distance $\lambda(\mathrm{Fo})$. The region $(1-\lambda, 1)$ is divided into k equal subregions. Assuming a fix $\mathrm{Fo}^* = \mathrm{Fo} > 0$, the elements of matrix X are computed by solving the Sylvester equation (28). The interface

condition (14) is used to evaluate the generalized time Fo^*. By replacing the space derivative by its average value and then integrating with respect to Fo from 0 to Fo, we obtain

$$\lambda(\mathrm{Fo}) = \frac{1}{20h} \cdot \int_0^{\mathrm{Fo}} (21 - 13\theta_k - 17\theta_{k-1} + 9\theta_{k-2})\,\mathrm{dFo}. \tag{29}$$

5. Numerical Computation and Discussion

The above solutions are of interest as they describe the inward solidification process of a melt in different geometries such as slab, circular cylinder or sphere when the surface is subjected under most generalized boundary condition. To analyze the solution, we consider particular cases of technical importance. In general, it is categorized into the following three different modalities:

Case 1. The surface is subjected to a boundary condition of first kind. In this case, we take

$$A' = 0,\ B' = 1,\quad (\mathrm{I})\ \theta_c(\mathrm{Fo}) = 0,\ (\mathrm{II})\ \theta_c = \mathrm{PdFo}, \tag{30}$$

where Pd is the Predvoditelev number defined as $\mathrm{Pd} = \frac{bR^2}{a\Delta T}$.

Case 2. The second kind boundary condition consists in assigning heat flux at the surface. In this case, we take

$$A' = 1,\ B' = 0,\quad \theta_c(\mathrm{Fo}) = \mathrm{Ki}(\mathrm{Fo}) = \mathrm{Ki}\,e^{(-\mathrm{PdFo})}, \tag{31}$$

where Ki is the Kirpichev number defined as $\mathrm{Ki} = \frac{ql}{k\Delta T}$.

Case 3. The third kind boundary conditions generally characterize the law of convective heat transfer between the surface of a body and its surrounding for a constant heat flux. In this case, we take

$$A' = 1,\ B' = \mathrm{Bi},\quad \theta_c(\mathrm{Fo}) = 0. \tag{32}$$

where Bi is the Biot number defined as $\mathrm{Bi} = \frac{\alpha R}{K}$.

The computation has been made and the results are presented in tables and eighteen figures. On the figures presented in this study, only the parameters whose values are different from the reference values are indicated. The selected reference values include Pd = 1.0, Ki = 1.0, Bi = 1.0, Fo = 1.0. The dimensionless temperature θ, at the end of solidification process, as a function of space coordinate for slab, circular cylinder, and sphere for boundary condition of first and second kind are shown in Figures 1–4, respectively. In third kind of boundary condition the temperature θ for slab, circular cylinder, and sphere are arranged in Table 1. The solid region thickness as a function of generalized time Fo for different Γ under boundary condition of first and second kind are depicted in Figures 5 and 6, respectively. A slab takes time Fo = 0.0578, a circular cylinder Fo = 0.0644, and a sphere Fo = 0.0736 when the surface is subjected to boundary conditions of first kind. When the

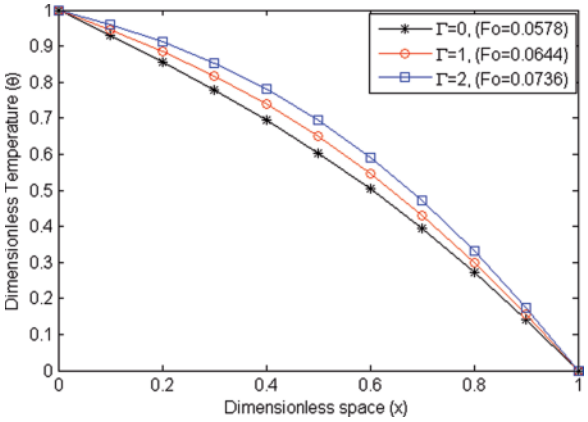

Fig. 1 (colour online). Temperature distribution in boundary condition of first kind (I).

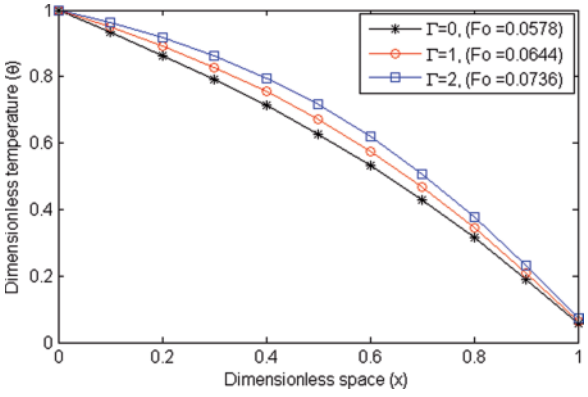

Fig. 2 (colour online). Temperature distribution in boundary condition of first kind, Pd = 1.0 (II).

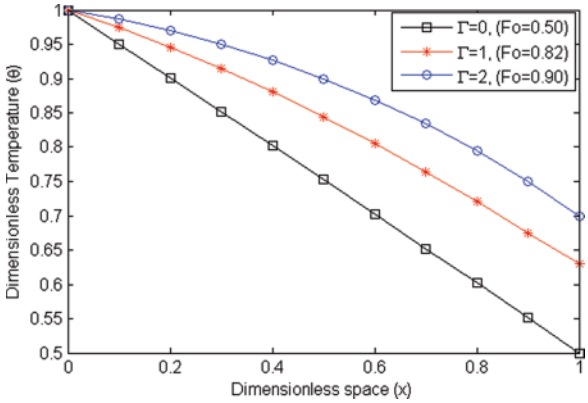

Fig. 3 (colour online). Temperature distribution in boundary condition of second kind, Ki = 1.0 (I).

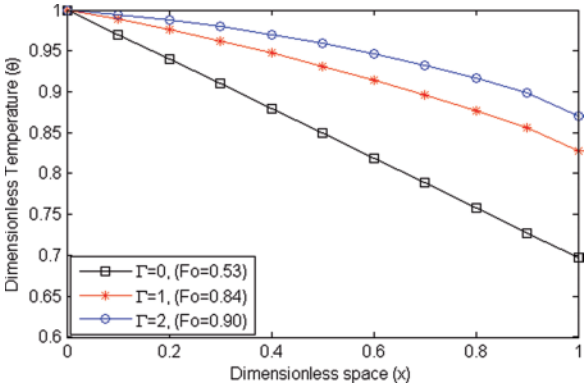

Fig. 4 (colour online). Temperature distribution in boundary condition of second kind, Ki = 1.0, Pd = 1.0 (II).

surface is subjected to boundary conditions of second kind, slab takes Fo = 0.50, cylinder takes Fo = 0.82, and sphere takes Fo = 0.90. When the surface is subjected to boundary conditions of third kind as shown in Table 1, slab takes time Fo = 0.88, cylinder takes Fo = 0.90, and sphere takes Fo = 0.92. In basic equation of heat conduction in a simple body like an infinite plate, circular cylinder or sphere, the term $\frac{\partial T}{\partial t}$ represents the rate of change of temperature with respect to time and can be replaced by $\frac{\delta T_t}{t}$. Similarly, $\frac{\partial T}{\partial x}$ represents the rate of change of temperature with respect to x and can be replaced by $\frac{\delta T_R}{x}$. The term $\frac{\partial^2 T}{\partial x^2}$ is the square rate of change of T with respect to x, and it can be replaced by $\frac{\delta T_R}{x^2}$, where the suffixes t and R denote the time rate and space rate change in temperature T. Therefore, the heat conduction equation reduces to

$$\frac{\delta T_t}{t} = a\left(\frac{\delta T_R}{R^2} + \frac{\Gamma}{R}\frac{\delta T_R}{R}\right), \tag{33}$$

i.e

$$\frac{1}{(1+\Gamma)}\frac{\delta T_t}{\delta T_R} = \frac{at}{R^2}. \tag{34}$$

The right hand side of this equation, being a dimensionless quantity, is called Fourier number or solidification time Fo = $\frac{at}{R^2}$. Thus, the Fourier number is defined as the ratio of time rate change in temperature with the space rate change in temperature, i.e.

$$\mathrm{Fo} = \frac{1}{(1+\Gamma)}\frac{\delta T_t}{\delta T_R}. \tag{35}$$

Table 1. Effect of temperature (θ) for third kind of boundary condition.

Γ	0	1	2
Fo	0.88	0.90	0.92
x	θ	θ	θ
0	1	1	1
0.1	0.77751	0.78181	0.78613
0.2	0.55521	0.56137	0.56760
0.3	0.33328	0.33887	0.34448
0.4	0.11190	0.11449	0.11684
0.5	0.10873	0.11160	0.11528
0.6	0.10628	0.10937	0.11412
0.7	0.10454	0.10778	0.11335
0.8	0.10348	0.10683	0.11299
0.9	0.10309	0.10652	0.11305
1.0	0.0958	0.0958	0.0958

Table 2. Effect of Bi on moving layer thickness $\lambda, S = 1.0$.

Γ	0	0	0	1	1	1	2	2	2
Bi	0.2	0.4	0.6	0.2	0.4	0.6	0.2	0.4	0.6
Fo	λ	λ	λ	λ	λ	λ	λ	λ	λ
0.00	0.00000	0.00000	0.00000	0.00000	0.00000	0.00000	0.00000	0.00000	0.00000
0.01	0.22019	0.22022	0.22026	0.21465	0.21468	0.21472	0.20916	0.20920	0.20923
0.02	0.44092	0.44099	0.44106	0.42985	0.42992	0.42999	0.41890	0.41896	0.41903
0.03	0.66210	0.66221	0.66232	0.64552	0.64562	0.64572	0.62911	0.62920	0.62929
0.04	0.88366	0.88380	0.88394	0.86158	0.86170	0.86183	0.83971	0.83983	0.83995

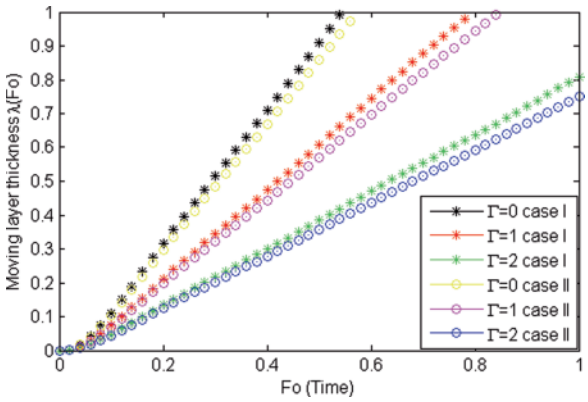

Fig. 5 (colour online). Moving layer thickness $\lambda(\mathrm{Fo})$ for boundary condition of first kind, $S = 1$ (I).

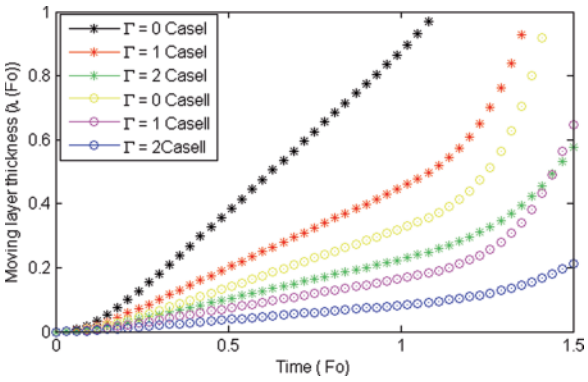

Fig. 6 (colour online). Moving layer thickness $\lambda(\mathrm{Fo})$ for boundary condition of second kind, $S = 1$ (II).

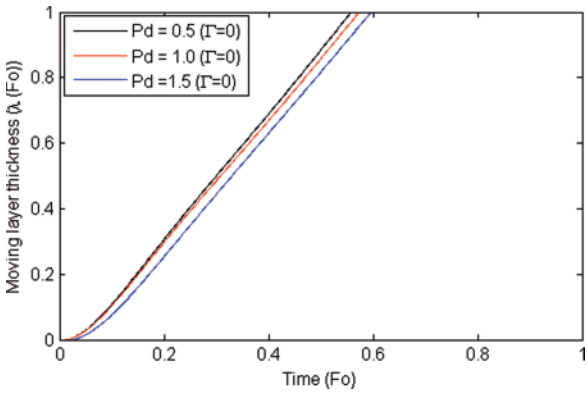

Fig. 7 (colour online). Effect of Pd on moving layer thickness $\lambda(\mathrm{Fo})$ for boundary condition of first kind, $S = 1$ (II).

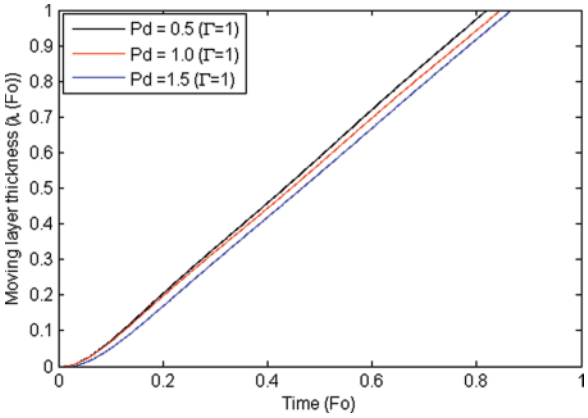

Fig. 8 (colour online). Effect of Pd on moving layer thickness $\lambda(\mathrm{Fo})$ for boundary condition of first kind, $S = 1$ (II).

Thus, the ratio of time rate change in temperature with the space rate change in temperature increases as shape factor Γ and Fourier number increase. This ratio is highest in a sphere and lowest in a plate. The temperature in a sphere is highest and in a plate is lowest in all types of boundary conditions. It is evident from Figures 5 and 6 that the moving layer thickness in a slab is highest while in a sphere is lowest and because of this the time taken for complete freezing in a slab is lowest and in a sphere is highest. In Case 3, when the surface is subjected to boundary condition of third kind, as Biot number increases, the temperature of the solid region decreases (Tab. 1) while the solid layer thickness increases (Tab. 2). The Biot number provides a way to compare the conduction resistance within a solid body with the convection resistance external to that body for heat transfer. It provides a way to use a proper method of analysis for appropriate situations. The process is fastest in the boundary condition of first kind in comparison to boundary condition of second and third kind. It is due to the fact that in the boundary condition of first kind, Bi is infinity, in boundary condition of second kind $\mathrm{Bi} = \frac{1}{\theta}$, while in boundary condition of third kind, it is finite. The dynamics of propagation of the freezing front during the freezing process for Bi infinite are different from those in the process where Bi is finite. In a freezing process with infinite Bi, the front starts advancing into the liquid with infinite speed, whereas in a freezing process with finite Bi, the front starts advancing into the liquid with a vanishing front speed. This is the reason why the freezing process is fastest in boundary condition of first kind in comparison to boundary conditions of second and third kind.

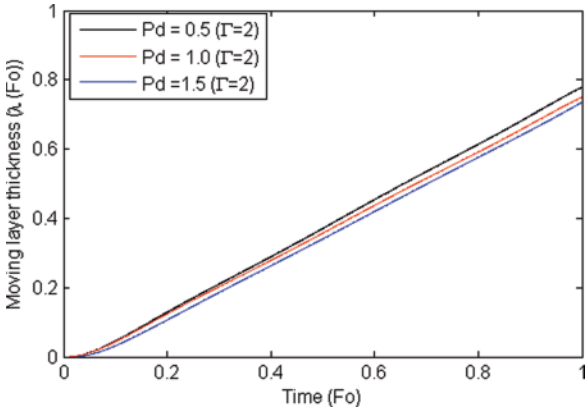

Fig. 9 (colour online). Effect of Pd on moving layer thickness $\lambda(\mathrm{Fo})$ for boundary condition of first kind, $S = 1$ (II).

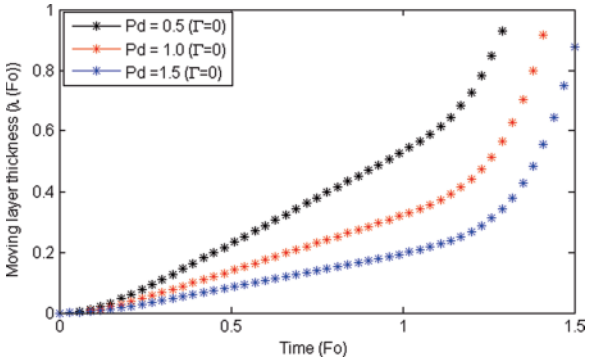

Fig. 10 (colour online). Effect of Pd on moving layer thickness $\lambda(\mathrm{Fo})$ for boundary condition of second kind, $K = 1.0$, $S = 1$ (II).

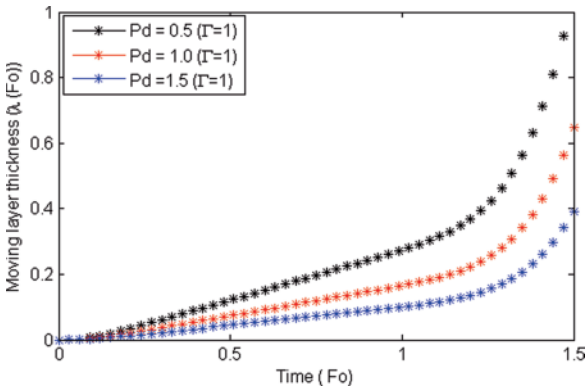

Fig. 11 (colour online). Effect of Pd on moving layer thickness $\lambda(\mathrm{Fo})$ for boundary condition of second kind, $\mathrm{Ki} = 1.0$, $S = 1$ (II).

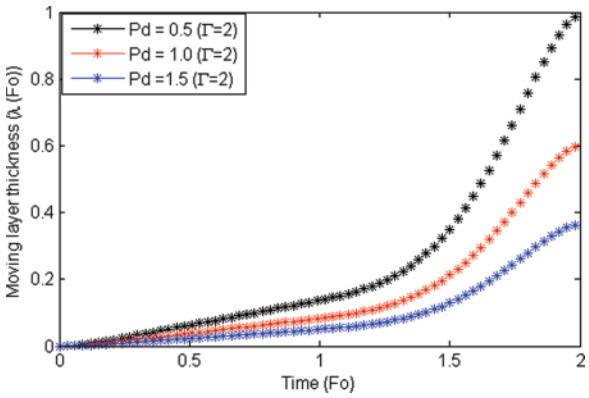

Fig. 12 (colour online). Effect of Pd on moving layer thickness $\lambda(\mathrm{Fo})$ for boundary condition of second kind, $\mathrm{Ki} = 1.0$, $S = 1$ (II).

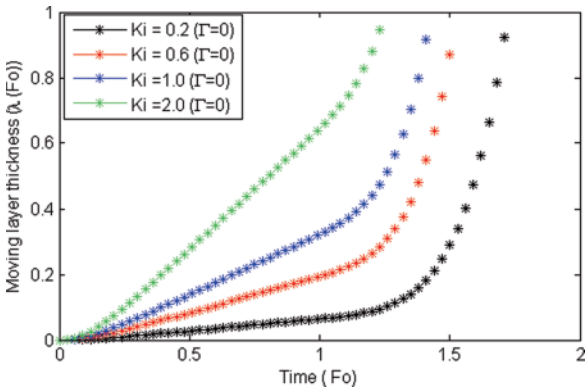

Fig. 13 (colour online). Effect of Ki on moving layer thickness $\lambda(\mathrm{Fo})$ for boundary condition of second kind, $\mathrm{Pd} = 1.0$, $S = 1$.

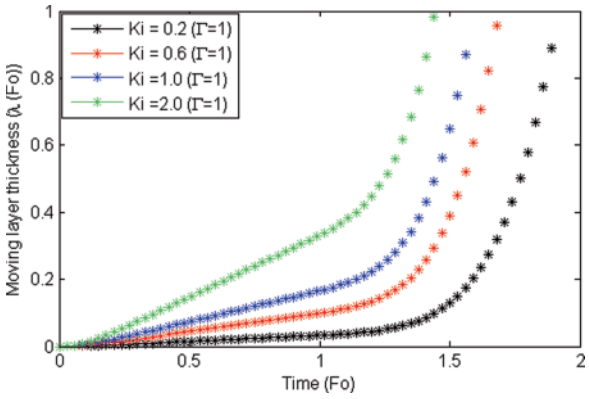

Fig. 14 (colour online). Effect of Ki on moving layer thickness $\lambda(\mathrm{Fo})$ for boundary condition of second kind, $\mathrm{Pd} = 1.0$, $S = 1$.

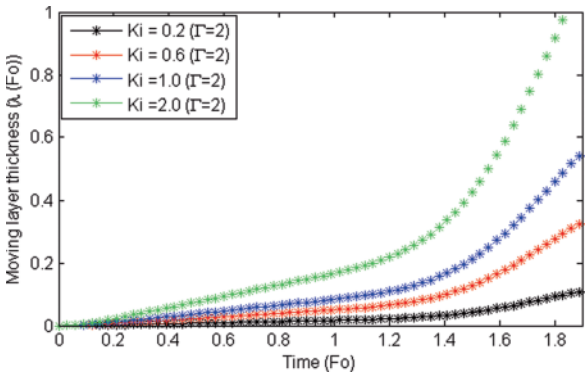

Fig. 15 (colour online). Effect of Ki on moving layer thickness $\lambda\,(\mathrm{Fo})$ for boundary condition of second kind, $\mathrm{Pd} = 1.0$, $S = 1$.

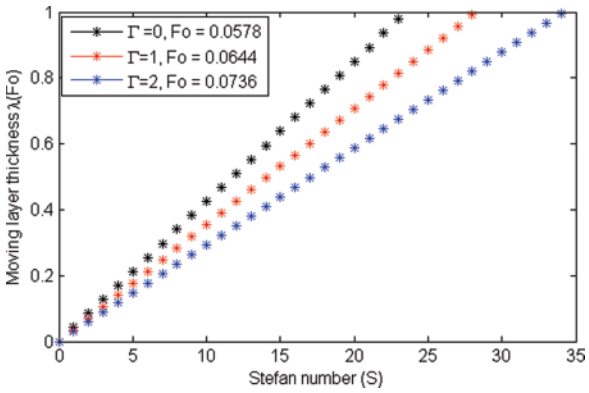

Fig. 16 (colour online). Effect of Stefan number on moving layer thickness $\lambda\,(\mathrm{Fo})$ for boundary condition of first kind.

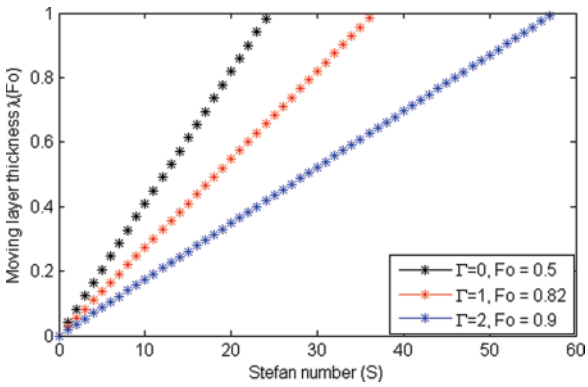

Fig. 17 (colour online). Effect of Stefan number on moving layer thickness $\lambda\,(\mathrm{Fo})$ for boundary condition of second kind.

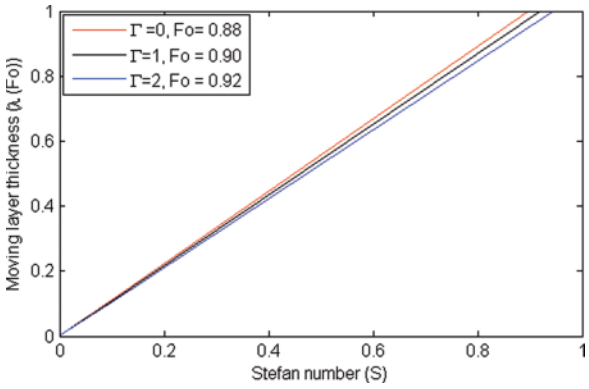

Fig. 18 (colour online). Effect of Stefan number on moving layer thickness $\lambda\,(\mathrm{Fo})$ for boundary condition of third kind.

As the Stefan number increases, the dimensionless solid layer thickness increases, and the time of complete solidification decreases. This time is minimum in slab and maximum in sphere. When the Stefan number decreases and approaches zero, the dimensionless solid layer thickness also decreases and is tending to zero. The Stefan number signifies the importance of sensible heat relative to the latent heat. A higher value of heat capacity or higher ΔT (in boundary condition of first kind $\Delta T = T_{\mathrm{f}} - T_{\mathrm{o}}$, in boundary condition of second kind $\Delta T = \frac{ql}{K}$, in boundary condition of third kind $\Delta T = T_{\mathrm{f}} - T_{\infty}$) or a lower value of latent heat accelerates the freezing process as shown in Figures 16 – 18, respectively. As the Stefan number increases, the time required for complete solidification decreases and approaches zero. In such situations the solidification process may be so rapid that liquid molecules have no time to rearrange themselves into the usual crystal structure and instead form an amorphous solid structure that is reminiscent of the liquid phase. For this reason solid formed from a supercooled liquid have been referred to as liquid of pause [21].

6. Conclusion

A continuum model for the inward solidification of a melt in different geometries under most generalized boundary conditions has been presented. The finite element Legendre wavelet Galerkin method (FELWGM) has been used to obtain the solution of this moving boundary problem. It can be seen that the proposed method is efficient and accurate to determine the solution of the moving boundary problem. In view of the excellent convergence of the Legendre wavelet se-

ries, only a few terms of the series are needed to give satisfactory results. The finite element method minimizes the error at each point. The exceptional accuracy prompts us to conclude that FELWGM may be an excellent alternative of other methods for solving boundary value problems containing two nonlinearities. Our simulation show that

- during solidification the dimensionless temperature is highest in a sphere and lowest in a slab while it is in between them in a cylinder;
- the solidification process is fastest in a slab and slowest in a sphere while it is in between them in a cylinder;
- the solidification process is fastest in boundary conditions of first kind in comparison to boundary conditions of second and third kind;
- the solidification process increases as the Predvoditelev number Pd decreases;
- the solidification process increases as the Kirpichev number Ki or the Biot number Bi increases;
- the solidification process increases as the Stefan number increases.

[1] F. L. Kennard, R. C. Bradt, and V. S. Stubican, Amer. Cera. Soci. **57**, 428 (1974).
[2] J. Crank, Free and Moving Boundary Problems, Oxford University Press, Oxford, UK 1984.
[3] R. H. Tien and G. E. Geiger, Trans. ASME, J. Heat Trans. **89**, 230 (1967).
[4] H. S. Carslaw and J. C . Jaegar, Conduction of Heat in Solids, Oxford University Press, Oxford, London 1959.
[5] M. N. Ozisik, Heat Conduction, Willey, New York 1993.
[6] J. M. Hill, One Dimensional Stefan Problem, John Willy and Sons Inc., New York 1987.
[7] R. Viskanta, Trans. ASME, J. Heat Trans. **110**, 1205 (1988).
[8] G. W. Barry and J. S. Goodling, Trans. ASME, J. Heat Trans. **109**, 820 (1987).
[9] J. S. Goodling and M. S. Khader, Trans. ASME, J. Heat Trans. **96**, 114 (1974).
[10] S. C. Gupta and P. R. Arora, Int. J. Heat Mass Trans. **30**, 2611 (1987).
[11] M. M. Yan and P. N. S. Huang, Trans. ASME, J. Heat Trans. **96**, 95 (1974).
[12] Y. P. Shih and T. C. Chou, Chem. Eng. Sci. **26**, 1787 (1971).
[13] K. N. Rai and D. C. Rai, Proceeding 4th National Confer. Ther. Sys. IT (BHU), pp. 259–267, Varanasi, India 2003.
[14] J. M. Hill and A. Kucera, Int. J. Heat and Mass Trans. **26**, 1631 (1983).
[15] K. A. R. Ismail and J. R. Henriquez, Ener. Conser. Manag. **41**, 173 (2000).
[16] L. Bilir and I. Zafer, J. Appl. Ther. Eng. **25**, 1488 (2005).
[17] C. W. Chan and F. L. Tan, Int. Commun. Heat Mass Trans. **33**, 335 (2006).
[18] F. L. Tan and K. C. Leong, Material Process. Tech. **89**, 159 (1999).
[19] M. Razzaghi and S. Yousefi, Math. Comput. Simul. **55**, 185 (2000).
[20] M. Razzaghi and S. Yousefi, Int. J. Sys. Sci. **32**, 495 (2001).
[21] NASA, NASA Science News: liquids on pause, http://science.nasa.gov/science-news/science-at-nasa/2003/16octviscocity/2003, 12 May 2012.